Konuralp Journal of Mathematics, 13 (1) (2025) 67-77

Konuralp Journal of Mathematics

Research Paper

Journal Homepage: www.dergipark.gov.tr/konuralpjournalmath

e-ISSN: 2147-625X

Mathematical Analysis of A Fractional-Order Viral Infection Model with Saturated Infection Rate and Cellular Immune Response

Jaouad Danane[1], **Mehmet Yavuz**[2,3,*] **and Sania Qureshi**[4,5,6]

[1]*Laboratory of Mathematics and Applications, Faculty of Sciences and Technologies, University Hassan II of Casablanca, PO Box 146, 20650, Mohammedia, Morocco*

[2]*Department of Mathematics and Computer Sciences, Faculty of Science, Necmettin Erbakan University, Meram Yeniyol, 42090 Konya, Türkiye*

[3]*Department of Applied Mathematics and Informatics, Kyrgyz-Turkish Manas University, Bishkek 720038, Kyrgyzstan*

[4]*Department of Basic Sciences and Related Studies, Mehran University of Engineering & Technology, Jamshoro – 76062, Pakistan*

[5]*Near East University, Mathematics Research Center, Department of Mathematics, Near East Boulevard, PC: 99138, Nicosia Mersin 10 – Turkey*

[6]*Research Center of Applied Mathematics, Khazar University, Baku, Azerbaijan*

[*]*Corresponding author*

Abstract

This paper investigates a fractional-order viral infection model with saturated infection rate and cellular immune response. The cellular immunity will be represented by cytotoxic T-lymphocytes (CTL) cells. In order to study mathematically the infection model, we will suggest five fractional differential equations describing the interaction between the uninfected cells, the latently infected cells, the infected cells, the CTL cells and the free viruses. A saturated infection rate will be taken into consideration to represent the viral infection. First, the positivity and boundedness of solutions for non-negative initial data are proved. Next, by constructing suitable Lyapunov functions, the global stability of the disease free equilibrium and the endemic equilibria are established depending on the basic reproduction number R_0 and the CTL immune response reproduction number R_{CTL}. Finally, numerical simulations are performed in order to show the dynamics behavior of the viral infection and to support the theoretical results.

Keywords: *Global stability; viral dynamics; CTL immune response; viral infection model; fractional derivative*

2010 Mathematics Subject Classification: *65L05, 34K06, 34K28*

1. Introduction

Infectious diseases are one of the major public health problems [1]. Accordingly, significant advances in this subject are deployed in treatment and control of the diseases spread. Among the most dangerous, the human immunodeficiency virus (HIV) which is known as a pathogen that attacks the immune system [2, 3], the hepatitis C virus (HCV) and the hepatitis B virus (HBV) that attack liver cells [4, 5, 6] and the human papillomavirus (HPV) that infects basal cells of the cervix [7, 8] and is highly correlated with the risk of developing cervical cancer and genital warts [9]. The modeling of viral infection becomes an important tool to predict and analyze the behavior of the infection [10, 11, 12]. The first viral infection model presented by Nowak and Bangham in 1996 studied the interaction between the uninfected cells, the infected cells and the free virus [10]. In 2012, Buonomo and Vargas-De-Leon decompose the infect class into two classes that represent the infected cells in latent stage and one other in active phase [13]. Recently, Sun et al. [14] suggested a modified model of Buonomo and Vargas-De-Leon by considering a saturated infection rate, this rate is more realistic than the mass action one since it describes the virus crowd near the uninfected cell [15, 14, 16]. On the other hand, it is well known that the cellular immune response plays an essential role to control the viral infection by killing the infected cells [16, 17, 18, 19, 20, 21, 22]. For instance, in a recent work, Allali et al. [16] add the component that represents the cellular immunity into the model already presented by Sun et al. [14] and show how the immunity participates in reducing viral replication.

Nowadays, fractional calculus is one of the better mathematical tools to characterize the memory of many complex systems [23, 24]. Indeed, hereditary and memory in several evolutionary problems need to be modeled via fractional derivatives. In particular, the mathematical

Email addresses: **jaouaddanane@gmail.com (Jaouad Danane), mehmetyavuz@erbakan.edu.tr (Mehmet Yavuz), sania.qureshi@faculty.muet.edu.pk (Sania Qureshi)**

modeling in biological systems requires time-fractional derivative since the dynamics of each biological component depends on the previous history of its proper evolution [25, 26, 27]. Therefore, fractional order differential modeling is better than the integer order one to describe the dynamics of many natural phenomena that can happen in physics, chemistry and biochemistry, hydrology, medicine and finance [28, 29, 30, 31, 32, 33, 34]. Recent studies have shown that fractional derivatives play a significant role in accurately modeling the propagation and dynamics of infectious diseases. Unlike classical integer-order models, fractional-order models incorporate memory and hereditary properties, which are essential for capturing the complex behavior of real-world epidemiological systems. These models have proven particularly effective in describing the long-term behavior of disease spread, latency periods, and immune responses. The use of fractional calculus enables researchers to better fit empirical data and account for anomalous diffusion and sub-exponential growth patterns often observed in real outbreaks. Furthermore, fractional models provide deeper insights into the effectiveness of control strategies, such as vaccination and quarantine, by reflecting how past states influence current dynamics. As a result, the inclusion of fractional derivatives enhances the predictive power and realism of infectious disease models, offering valuable tools for public health planning and response [35, 36, 37, 38, 39, 40, 41, 42, 43, 44, 45]. Motivated by the previous works, we extend in this study the recent work presented in [16] by using the fractional order derivatives in each model component. The model that we suggest is given by the following nonlinear system:

$$\begin{cases} D^{\alpha}x = \lambda - d_1 x - \dfrac{k_1 xv}{x+v}, \\ D^{\alpha}s = \dfrac{k_1 xv}{x+v} - d_2 s - k_2 s, \\ D^{\alpha}y = k_2 s - d_3 y - pyz, \\ D^{\alpha}v = ay - d_4 v, \\ D^{\alpha}z = cyz - bz. \end{cases} \tag{1.1}$$

With the initial conditions $x(0) = x_0$, $s(0) = s_0$, $y(0) = y_0$, $v(0) = v_0$ and $z(0) = z_0$. The Caputo fractional derivative of order $\alpha > 0$ is defined as follows :

$$D^{\alpha}\psi(t) = \frac{1}{\Gamma(1-\alpha)} \int_0^t \frac{\psi'(s)}{(t-s)^{\alpha}} ds, \tag{1.2}$$

where $\Gamma(.)$ is Gamma function.
In this model, x, y, s, v and z denote the concentration of uninfected cells, infected cells, exposed cells, free virus and CTL cells, respectively. Susceptible host cells are produced at a rate λ, die at a rate $d_1 x$ and become infected by virus at a rate $\frac{k_1 xv}{x+v}$. Exposed cells die at a rate $d_2 s$ and become infected at a rate of $k_2 s$. Infected cells increase at rate $k_2 s$, die at rate $d_3 y$ and are killed by the CTL response at a rate pyz. Free virus is produced by infected cells at a rate ay and decays at a rate $d_4 v$. Finally, CTLs expand in response to viral antigen derived from infected cells at a rate cyz and decay in the absence of antigenic stimulation at a rate bz. In this paper, we will study this new fractional derivative model (1.1) taking into account the memory in each viral infection component. We will check the impact of the fractional derivative order on the stability of viral infection equilibria.
The rest of the paper is organized as follows. In Section 2, deals with some basic proprieties of the solution and the steady states result. In Section 3, the global stability of each steady states is established. Numerical simulations are presented in Section 4 to support the theoretical findings. Concluding remarks are given in the last section.

2. Positivity, boundedness and equilibria

2.1. Positivity and boundedness

For the problems dealing with biological cell dynamics, the cell densities should remain non-negative and bounded. In this subsection, we will establish the positivity and boundedness of solutions of the model (1.1). First of all, for biological reasons, the parameters x_0, s_0, y_0, v_0 and z_0 must be larger than or equal to 0. For the existence, positivity and boundedness of the problem solution, we have the following result:

Proposition 2.1. *For any non-negative initial conditions $(x_0, s_0, y_0, v_0, z_0)$, the system (1.1) has a unique solution. Moreover, this solution is non-negative and bounded for all $t \geq 0$.*

Proof. First, the model (1.1) can be rewritten as follows:

$$D^{\alpha}X = B + A_1 X + yA_2 X + \frac{v}{x+v} A_3 X, \tag{2.1}$$

where

$$X = \begin{pmatrix} x \\ s \\ y \\ v \\ z \end{pmatrix}, \quad B = \begin{pmatrix} \lambda \\ 0 \\ 0 \\ 0 \\ 0 \end{pmatrix},$$

$$A_1 = \begin{pmatrix} -d_1 & 0 & 0 & 0 & 0 \\ 0 & -(d_2+k_2) & 0 & 0 & 0 \\ 0 & k_2 & -d_3 & 0 & 0 \\ 0 & 0 & a & d_4 & 0 \\ 0 & 0 & a & 0 & b \end{pmatrix},$$

$$A_2 = \begin{pmatrix} 0 & 0 & 0 & 0 & 0 \\ 0 & 0 & 0 & 0 & 0 \\ 0 & 0 & 0 & 0 & -p \\ 0 & 0 & 0 & 0 & 0 \\ 0 & 0 & 0 & 0 & c \end{pmatrix}$$

and

$$A_3 = \begin{pmatrix} -k_1 & 0 & 0 & 0 & 0 \\ k_1 & 0 & 0 & 0 & 0 \\ 0 & 0 & 0 & 0 & 0 \\ 0 & 0 & 0 & 0 & 0 \\ 0 & 0 & 0 & 0 & 0 \end{pmatrix}.$$

From (2.1), we have

$$\| D^{\alpha} X \| \leq \| B \| + (\| A_1 \| + \| y \| \| A_2 \| + \| A_3 \|) \| X \|.$$

Hence, the conditions of Lemma 4 in [27] are satisfied. Therefore, the system (1.1) has a unique solution on $[0, +\infty)$.
Now, we will prove the nonnegativity of solution. First, we have

$$D^{\alpha} x \mid_{x=0} = \lambda \geq 0,$$

$$D^{\alpha} s \mid_{s=0} = \frac{k_1 x v}{x+v} \geq 0,$$

$$D^{\alpha} y \mid_{y=0} = k_2 s \geq 0,$$

$$D^{\alpha} v \mid_{v=0} = ay \geq 0$$

and

$$D^{\alpha} z \mid_{v=0} = 0 \geq 0,$$

this shows that the solution of system (1.1) is non-negative.
About the boundedness of the solutions; if we assume that

$$N = x + s + y + \frac{p}{c} z,$$

then, we will have

$$\begin{aligned} D^{\alpha} N(t) &= \lambda - d_1 x - d_2 s - d_3 y - \frac{bp}{c} z, \\ &\leq \lambda - \rho N(t), \end{aligned}$$

with $\rho = min\{d_1, d_2, d_3, b\}$. Therefore

$$N(t) \leq N(0) E_{\alpha}(-\rho t^{\alpha}) + \frac{\lambda}{\rho} \left((1 - E_{\alpha}(-\rho t^{\alpha})) \right),$$

where $E_{\alpha}(u) = \sum_{j=0}^{+\infty} \frac{u^j}{\Gamma(\alpha j + 1)}$ is the Mittag-Leffler function of parameter α.
Since $0 \leq E_{\alpha}(-\rho t^{\alpha}) \leq 1$, then

$$N(t) \leq N(0) E_{\alpha}(-\rho t^{\alpha}) + \frac{\lambda}{\rho}.$$

This fact, implies that x, s, y and z are bounded.
Using the fourth equation of system (1.1), we will have

$$v(t) \leq v(0) + \frac{a}{d_4} \| y \|_{\infty}.$$

then the last variable of the problem v is also bounded. □

2.2. Disease free equilibrium and endemic equilibria

The system (1.1) has a disease-free equilibrium $E_f = (\frac{\lambda}{d_1}, 0, 0, 0, 0)$, corresponding to the maximal level of healthy cells. The basic reproduction number of our model is given as follows:

$$R_0 = \frac{ak_1k_2}{d_3d_4(d_2+k_2)}, \tag{2.2}$$

In addition to the disease-free equilibrium, the system (1.1) admits three endemic equilibria. The first of them is $E_1 = (x_1, s_1, y_1, v_1, 0)$ called the free-immune endemic equilibrium, where

$$\begin{aligned} x_1 &= \frac{\lambda}{d_1 + k_1(1-\frac{1}{R_0})}, \\ s_1 &= \frac{k_1\lambda(R_0-1)}{(d_2+k_2)(R_0d_1+k_1(R_0-1))}, \\ y_1 &= \frac{d_4\lambda(R_0-1)}{ad_1+ak_1(1-\frac{1}{R_0})}, \\ v_1 &= \frac{\lambda(R_0-1)}{d_1+k_1(1-\frac{1}{R_0})}. \end{aligned}$$

The second endemic steady state is $E_2 = (x_2, s_2, y_2, v_2, z_2)$ called the infection equilibrium with immunity, where

$$\begin{aligned} x_2 &= \frac{-abd_1 - abk_1 + \lambda cd_4 + \sqrt{A}}{2cd_1d_4}, \\ s_2 &= \frac{d_3R_0}{k_2}\frac{b(-abd_1 - abk_1 + \lambda cd_4 + \sqrt{A})}{c(abd_1 - abk_1 + \lambda cd_4 + \sqrt{A})}, \\ y_2 &= \frac{b}{c}, \\ v_2 &= \frac{ba}{cd_4}, \\ z_2 &= \frac{d_3((R_0-1)(-ak_1b + \lambda cd_4 + \sqrt{A}) - abd_1(R_0+1))}{p(abd_1 - ak_1b + \lambda cd_4 + \sqrt{A})}. \end{aligned}$$

The third infection steady state is $E_3 = (x_3, s_3, y_3, v_3, z_3)$, where

$$\begin{aligned} x_3 &= -\frac{abd_1 + abk_1 - \lambda cd_4 + \sqrt{A}}{2cd_1d_4}, \\ s_3 &= \frac{k_1x_3v_3}{(k_2+d_2)(x_3+v_3)}, \\ y_3 &= \frac{b}{c}, \\ v_3 &= \frac{ba}{cd_4}, \\ z_3 &= \frac{k_2s_3 - d_3y_3}{py_3}, \end{aligned}$$

with $A = (abk_1 - \lambda cd_4)^2 + a^2b^2d_1^2 + 2a^2b^2d_1k_1 + 2\lambda abcd_1d_4$.

- Since $x_3 < 0$, the last infection steady state E_3 will not be taken into consideration.
- From the components of E_1, it is clear that when $R_0 > 1$, this endemic point exists.
- In order to classify the dynamics of our model, we define the following CTL immune response reproduction number

$$R_{CTL} = \frac{cy_1}{b} = \frac{cd_4\lambda R_0(1-\frac{1}{R_0})}{abd_1 + abk_1(1-\frac{1}{R_0})}.$$

It is clear that the second endemic state E_2 exists when $R_{CTL} > 1$.

3. Global stability results

In this subsection, we study the global stability of each equilibrium. To this end, we will construct an appropriate Lyapunov functional for each case.
Fist, we will study the global stability of the disease-free equilibrium.

Proposition 3.1. *The free-infection equilibrium E_f is globally stable when $R_0 \leq 1$.*

Proof. Let's consider the following Lyapunov function:

$$\mathscr{L}(x,y,s,v,z) = s + \frac{d_2+k_2}{k_2}y + \frac{d_3(d_2+k_2)}{ak_2}v + \frac{p}{c}\frac{d_2+k_2}{k_2}z.$$

Then,

$$\begin{aligned}
D^\alpha \mathscr{L}(x,y,s,v,z) &= D^\alpha s + \frac{d_2+k_2}{k_2}D^\alpha y + \frac{d_3(d_2+k_2)}{ak_2}D^\alpha v + \frac{p}{c}\frac{d_2+k_2}{k_2}D^\alpha z.\\
D^\alpha \mathscr{L}(x,y,s,v,z) &= \frac{k_1 xv}{x+v} - (d_2+k_2)s + \frac{d_2+k_2}{k_2}(k_2 s - d_3 y) - \frac{d_2+k_2}{k_2}pyz + \frac{d_3(d_2+k_2)}{ak_2}(ay-d_4 v) + \frac{p}{c}\frac{d_2+k_2}{k_2}(cyz-bz)\\
D^\alpha \mathscr{L}(x,y,s,v,z) &= \frac{k_1 xv}{x+v} - \frac{d_3 d_4(d_2+k_2)}{ak_2}v - \frac{bp}{c}\frac{d_2+k_2}{k_2}z\\
D^\alpha \mathscr{L}(x,y,s,v,z) &\leq k_1 v - \frac{d_3 d_4(d_2+k_2)}{ak_2}v\\
&\leq \frac{d_3 d_4(d_2+k_2)}{ak_2}(R_0-1)v.
\end{aligned}$$

So $D^\alpha \mathscr{L} \leq 0$ when $R_0 < 1$. Moreover, $D^\alpha \mathscr{L} \leq 0$ when $v = 0$. The largest compact invariant is

$$E = \{(x,y,s,v,z) | v = 0\}.$$

So, $\lim_{+\infty} v(t) = 0$, the limit system of equations is

$$\begin{cases}
D^\alpha x = \lambda - d_1 x,\\
D^\alpha s = -d_2 s - k_2 s,\\
D^\alpha y = k_2 s - d_3 y - pyz,\\
D^\alpha z = cyz - bz.
\end{cases}$$

We define another Lyapunov function (for simplicity, we will use the same notation)

$$\mathscr{L}(x,s,y,z) = \frac{1}{x_0}\left(x - x_0 - x_0 \ln\frac{x}{x_0}\right) + s + \frac{d_2+k_2}{k_2}y + \frac{p}{c}\frac{d_2+k_2}{k_2}z.$$

Since $x_0 = \frac{\lambda}{d_1}$, we have

$$D^\alpha \mathscr{L}(x,s,y,z) \quad \leq d_1\left(2 - \frac{x}{x_0} - \frac{x_0}{x}\right) - \frac{d_3(d_2+k_2)}{k_2}y - \frac{pb}{c}z,$$

Using the fact that, the arithmetic mean is greater than or equal to the geometric mean, we have

$$2 - \frac{x}{x_0} - \frac{x_0}{x} \leq 0,$$

then $D^\alpha \mathscr{L} \leq 0$ and the equality holds if $x = x_0$ and $s = y = z = 0$, which prove the global stability of E_f. □

About the global stability of the free-immune endemic equilibrium E_1, we have the following result

Proposition 3.2. *If $R_0 > 1$ and $R_{CTL} \leq 1$, then the free-immune endemic equilibrium E_1 is globally stable.*

Proof. First, we use the following Lyapunov function:

$$\mathscr{L}_1(x,y,s,v,z) = x - x_1 - \int_{x_1}^{x}\frac{(d_2+k_2)s_1}{\frac{k_1 u v_1}{u+v_1}}du + s - s_1 - s_1\ln\frac{s}{s_1} + \frac{d_2+k_2}{k_2}(y - y_1 - y_1\ln\frac{y}{y_1}) + \frac{d_3(d_2+k_2)}{ak_2}(v - v_1 - v_1\ln\frac{v}{v_1}) + \frac{p}{c}\frac{d_2+k_2}{k_2}z.$$

Then,

$$D^\alpha \mathscr{L}_1(x,y,s,v,z) \quad \leq D^\alpha x - (d_2+k_2)s_1\frac{x+v_1}{k_1 x v_1}D^\alpha x + D^\alpha s - \frac{s_1}{s}D^\alpha s + \frac{d_2+k_2}{k_2}\left(1 - \frac{y_1}{y}\right)D^\alpha y + \frac{d_3(d_2+k_2)}{ak_2}\left(1 - \frac{v_1}{v}\right)D^\alpha v + \frac{p}{c}\frac{d_2+k_2}{k_2}D^\alpha z.$$

This fact implies that

$$\begin{aligned}
D^\alpha \mathscr{L}_1(x,s,y,v,z) &\leq \left(\lambda - d_1 x - \frac{k_1 xv}{x+v}\right)\left(1 - (d_2+k_2)s_1\frac{x+v_1}{k_1 x v_1}\right) + \frac{k_1 xv}{x+v} - (d_2+k_2)s - \frac{s_1}{s}\left(\frac{k_1 xv}{x+v} - (d_2+k_2)s\right)\\
&+ \frac{d_2+k_2}{k_2}(k_2 s - d_3 y - pyz) - \frac{d_2+k_2}{k_2}\frac{y_1}{y}(k_2 s - d_3 y - pyz) + \frac{d_3(d_2+k_2)}{ak_2}(ay - d_4 v) - \frac{d_3(d_2+k_2)}{ak_2}\frac{v_1}{v}(ay - d_4 v)\\
&+ \frac{p}{c}\frac{d_2+k_2}{k_2}(cyz - bz).
\end{aligned}$$

Since,

$$\begin{cases}
\lambda = d_1 x_1 + (d_2+k_2)s_1,\\
\frac{k_1 x_1 v_1}{x_1+v_1} = (d_2+k_2)s_1,\\
\frac{s_1}{v_1} = \frac{d_3 d_4}{ak_2},\ \frac{y_1}{v_1} = \frac{d_4}{a},\ \frac{s_1}{y_1} = \frac{d_3}{k_2}.
\end{cases}$$

We have

$$\begin{aligned} D^{\alpha}\mathscr{L}_1(x,s,y,v,z) &\leq \lambda - d_1x - (d_2+k_2)s_1\frac{x+v_1}{k_1xv_1}\left(\lambda - d_1x - \frac{k_1xv}{x+v}\right) - \frac{s_1}{s}\left(\frac{k_1xv}{x+v}\right) + (d_2+k_2)s_1 + \frac{d_2+k_2}{k_2}py_1z \\ &+ \frac{(d_2+k_2)d_3}{k_2}y_1 - (d_2+k_2)s\frac{y_1}{y} - \frac{d_3d_4(d_2+k_2)}{ak_2}v + \frac{d_3d_4(d_2+k_2)}{ak_2}v_1 - \frac{d_3(d_2+k_2)}{k_2}\frac{v_1y}{v} - \frac{d_2+k_2}{k_2}\frac{bp}{c}z. \end{aligned}$$

However, we know that

$$\begin{cases} \lambda - d_1x = d_1x_1 + (d_2+k_2)s_1 - d_1x, \\ \lambda - d_1x - (d_2+k_2)s_1\dfrac{x+v_1}{k_1xv_1}\left(\lambda - d_1x - \dfrac{k_1xv}{x+v}\right) = d_1x_1\left(1 - \dfrac{x}{x_1} - \dfrac{x_1}{x}\dfrac{x+v_1}{x_1+v_1} + \dfrac{x+v_1}{x_1+v_1}\right) + (d_2+k_2)s_1\left(1 - \dfrac{x_1}{x}\dfrac{x+v_1}{x_1+v_1} + \dfrac{v}{v_1}\dfrac{x+v_1}{x+v}\right), \\ -\dfrac{s_1}{s}\left(\dfrac{k_1xv}{x+v}\right) + (d_2+k_2)s_1 = -\dfrac{s_1}{s}\dfrac{xv}{x_1v_1}\dfrac{x_1+v_1}{x+v}(d_2+k_2)s_1 + (d_2+k_2)s_1, \end{cases}$$

then,

$$\begin{aligned} D^{\alpha}\mathscr{L}_1 &\leq d_1x_1\left(1 - \frac{x}{x_1} - \frac{x_1}{x}\frac{x+v_1}{x_1+v_1} + \frac{x+v_1}{x_1+v_1}\right) + (d_2+k_2)s_1\left(1 - \frac{x_1}{x}\frac{x+v_1}{x_1+v_1} + \frac{v}{v_1}\frac{x+v_1}{x+v}\right) \\ &+ (d_2+k_2)s_1\left(1 - \frac{s_1}{s}\frac{xv}{x_1v_1}\frac{x_1+v_1}{x+v}\right) + (d_2+k_2)s_1\left(1 - \frac{sy_1}{s_1y} - \frac{v}{v_1}\right) \\ &+ (d_2+k_2)s_1\left(1 - \frac{v_1y}{y_1v}\right) + pz\frac{d_2+k_2}{k_2}(y_1 - \frac{b}{c}). \end{aligned}$$

Therefore,

$$\begin{aligned} D^{\alpha}\mathscr{L}_1 &\leq -\frac{d_1v_1}{x(x_1+v_1)}(x-x_1)^2 + (d_2+k_2)s_1\left(-1 - \frac{v}{v_1} + \frac{v}{v_1}\frac{x+v_1}{x+v} + \frac{x+v}{x+v_1}\right) \\ &+ (d_2+k_2)s_1\left(5 - \frac{x_1}{x}\frac{x+v_1}{x_1+v_1} - \frac{s_1}{s}\frac{xv}{x_1v_1}\frac{x_1+v_1}{x+v} - \frac{sy_1}{s_1y} - \frac{yv_1}{y_1v} - \frac{x+v}{x+v_1}\right) + pz\frac{d_2+k_2}{k_2}(y_1 - \frac{b}{c}), \end{aligned}$$

As a result

$$\begin{aligned} D^{\alpha}\mathscr{L}_1 &\leq -\frac{d_1v_1}{x(x_1+v_1)}(x-x_1)^2 - (d_2+k_2)s_1\left(\frac{x(v-v_1)^2}{v_1(x+v_1)(x+v)}\right) \\ &+ (d_2+k_2)s_1\left(5 - \frac{x_1}{x}\frac{x+v_1}{x_1+v_1} - \frac{s_1}{s}\frac{xv}{x_1v_1}\frac{x_1+v_1}{x+v} - \frac{sy_1}{s_1y} - \frac{yv_1}{y_1v} - \frac{x+v}{x+v_1}\right) + p\frac{d_2+k_2}{k_2}\frac{b}{c}(R_{CTL}-1)z, \end{aligned}$$

since the arithmetic mean is greater than or equal to the geometric mean, then

$$5 - \frac{x_1}{x}\frac{x+v_1}{x_1+v_1} - \frac{s_1}{s}\frac{xv}{x_1v_1}\frac{x_1+v_1}{x+v} - \frac{sy_1}{s_1y} - \frac{yv_1}{y_1v} - \frac{x+v}{x+v_1} \leq 0.$$

When $R_{CTL} \leq 1$, we have $D^{\alpha}\mathscr{L}_1 \leq 0$, and the equality holds when $x = x_1$, $y = y_1$, $s = s_1$ and $v = v_1$. The free-immune endemic equilibrium E_1 is globally stable when $R_0 > 1$ and $R_{CTL} \leq 1$. □

Finally, the global stability result concerning the endemic equilibrium with immunity E_2 is given as follows

Proposition 3.3. *The endemic equilibrium with immunity E_2 is globally stable, when $R_0 > 1$ and $R_{CTL} > 1$.*

Proof. First, we define the following Lyapunov function

$$\begin{aligned} \mathscr{L}_2(x,s,y,v,z) &= x - x_2 - \int_{x_2}^{x}\frac{(d_2+k_2)s_2}{\frac{k_1uv_2}{u+v_2}}du + s - s_2 - s_2\ln\frac{s}{s_2} + \frac{d_2+k_2}{k_2}(y - y_2 - y_2\ln\frac{y}{y_2}) + \frac{d_3(d_2+k_2)+(d_2+k_2)pz_2}{ak_2} \\ &\times (v - v_2 - v_2\ln\frac{v}{v_2}) + \frac{p}{c}\frac{d_2+k_2}{k_2}(z - z_2 - z_2\ln\frac{z}{z_2}). \end{aligned}$$

Then

$$\begin{aligned} D^{\alpha}\mathscr{L}_2(x,y,s,v,z) \leq\ & D^{\alpha}x - (d_2+k_2)s_2\frac{x+v_2}{k_1xv_2}D^{\alpha}x + D^{\alpha}s - \frac{s_2}{s}D^{\alpha}s + \frac{d_2+k_2}{k_2}(D^{\alpha}y - \frac{y_2}{y}D^{\alpha}y) \\ &+ \frac{d_3(d_2+k_2)+(d_2+k_2)pz_2}{ak_2}(D^{\alpha}v - \frac{v_2}{v}D^{\alpha}v) + \frac{p}{c}\frac{d_2+k_2}{k_2}(D^{\alpha}z - \frac{z_2}{z}D^{\alpha}z). \end{aligned}$$

So,

$$\begin{aligned} D^{\alpha}\mathscr{L}_2(x,y,s,v,z) \leq\ & \lambda - d_1x - \frac{x_2}{x}\frac{x+v_2}{x_2+v_2}(\lambda - d_1x) + ((d_2+k_2)s_2)\frac{v}{v_2}\frac{x_2+v_2}{x+v} - (d_2+k_2)s \\ &- \frac{s_2}{s}\left(\frac{k_1xv}{x+v} - (d_2+k_2)s\right) + \frac{d_2+k_2}{k_2}(k_2s - d_3y - pyz) \\ &- \frac{d_2+k_2}{k_2}\frac{y_2}{y}(k_2s - d_3y - pyz) + \frac{d_3(d_2+k_2)+(d_2+k_2)pz_2}{ak_2} \\ &\times(ay - d_4v) - \frac{d_3(d_2+k_2)+(d_2+k_2)pz_2}{ak_2}\frac{v_2}{v}(ay - d_4v) \\ &+ \frac{p}{c}\frac{d_2+k_2}{k_2}(cyz - bz) - \frac{pz_2}{cz}\frac{d_2+k_2}{k_2}(cyz - bz). \end{aligned}$$

On the other hand, we have

$$\begin{cases} \frac{s_2}{y_2}=\frac{d_3}{k_2}+\frac{pz_2}{k_2},\ \frac{y_2}{v_2}=\frac{d_4}{a},\ \frac{s_2}{v_2}=\frac{d_3d_4}{ak_2}+\frac{d_4pz_2}{ak_2}, \\ \lambda-d_1x=d_1x_2+d_2+k_2)s_2-d_1x, \\ \lambda-d_1x-(d_2+k_2)s_2\frac{x+v_2}{k_1xv_2}\left(\lambda-d_1x-\frac{k_1xv}{x+v}\right)=d_1x_2(1-\frac{x}{x_2}-\frac{x_2}{x}\frac{x+v_2}{x_2+v_2} \\ \quad+\frac{x+v_2}{x_2+v2})+(d_2+k_2)s_2(1-\frac{x_2}{x}\frac{x+v_2}{x_2+v_2}+\frac{v}{v_2}\frac{x+v_2}{x+v}), \\ -\frac{s_2}{s}\left(\frac{k_1xv}{x+v}\right)+(d_2+k_2)s_2=(d_2+k_2)s_2(1-\frac{s_2}{s}\frac{xv}{x_2v_2}\frac{x_2+v_2}{x+v}) \end{cases}$$

and

$$\begin{cases} \frac{(d_2+k_2)d_3}{k_2}y_2-(d_2+k_2)s\frac{y_2}{y}-\frac{(d_2+k_2)d_3d_4}{ak_2}v \\ =(d_2+k_2)s_2\left(1-\frac{s}{s_2}\frac{y_2}{y}-\frac{v}{v_2}\right)+\frac{(d_2+k_2)}{k_2}pz_2y_2\frac{v}{v_2}-\frac{(d_2+k_2)}{k_2}pz_2y_2, \\ \frac{d_4d_3(d_2+k_2)}{ak_2}v_2-\frac{d_3(d_2+k_2)}{k_2}\frac{v_2}{v}y=(d_2+k_2)s_2\left(1-\frac{y}{y_2}\frac{v_2}{v}\right) \\ \quad+\frac{(d_2+k_2)}{k_2}pz_2y\frac{v_2}{v}-\frac{(d_2+k_2)}{k_2}pz_2y_2, \end{cases}$$

$$\begin{cases} \frac{(d_2+k_2)pz_2}{ak_2}(ay-d_4v)-\frac{(d_2+k_2)pz_2}{ak_2}\frac{v_2}{v}(ay-d_4v)=\frac{(d_2+k_2)pz_2y}{k_2} \\ \quad-\frac{(d_2+k_2)pz_2y_2}{k_2}\frac{v}{v_2}-\frac{(d_2+k_2)pz_2y}{k_2}\frac{v_2}{v}+\frac{(d_2+k_2)pz_2y_2}{k_2}, \\ \frac{(d_2+k_2)pz_2}{ak_2}(ay-d_4v)-\frac{(d_2+k_2)pz_2}{ak_2}\frac{v_2}{v}(ay-d_4v)-\frac{z_2}{z}\frac{p}{c}\frac{d_2+k_2}{k_2}(xyz-bz) \\ \quad+\frac{(d_2+k_2)}{k_2}pz_2y_2\frac{v}{v_2}-\frac{(d_2+k_2)}{k_2}pz_2y_2+\frac{(d_2+k_2)}{k_2}pz_2y\frac{v_2}{v}-\frac{(d_2+k_2)}{k_2}pz_2y_2=0. \end{cases}$$

Therefore, we have

$$\begin{aligned} D^\alpha\mathscr{L}_2(x,y,s,v,z)\leq & -\frac{d_1v_2}{x(x_2+v_2)}(x-x_2)^2 \\ & -(d_2+k_2)s_2\left(\tfrac{x(v-v_2)^2}{v_2(x+v_2)(x+v)}\right) \\ & +(d_2+k_2)s_2\left(5-\frac{x_2}{x}\frac{x+v_2}{x_2+v_2}-\frac{s_2}{s}\frac{xv}{x_2v_2}\frac{x_2+v_2}{x+v}-\frac{sy_2}{s_2y}-\frac{yv_2}{y_2v}-\frac{x+v}{x+v_2}\right), \end{aligned}$$

Also, since the arithmetic mean is greater than or equal to the geometric mean, we have

$$5-\frac{x_2}{x}\frac{x+v_2}{x_2+v_2}-\frac{s_2}{s}\frac{xv}{x_2v_2}\frac{x_2+v_2}{x+v}-\frac{sy_2}{s_2y}-\frac{yv_2}{y_2v}-\frac{x+v}{x+v_2}\leq 0,$$

which means that $D^\alpha\mathscr{L}_2\leq 0$, and the equality holds when $x=x_2$, $s=s_2$, $y=y_2$, $v=v_2$ and $z=z_2$. The endemic equilibrium with immunity E_2 is globally stable. □

4. Numerical simulations

In this section, we will perform some numerical simulations of the system (1.1) by using the parameters values from Table 1. The purpose of our numerical simulations will be to support our theoretical findings and to observe the impact of the fractional derivative order on the steady states stability.

Indeed, the first Fig. 4.1 shows the behavior of the viral dynamics during the first 80 days of the infection, for the parameters corresponding the stability of the free-disease equilibrium. We can see that all the curves corresponding to exposed cells, infected cells, virus and CTL cells vanish. However, the amount of the uninfected cells increases to reach its maximal level. This situation corresponds to the case of the disease-free equilibrium stability. More precisely, for the used parameters in this figure, we have the basic reproduction number is less than unity $R_0=0.2209<1$; we clearly see that, in this case, the solution of the system converge to the disease-free equilibrium point $E_f=(827.22,0,0,0,0)$. This numerical result is consistent with the theoretical result concerning the stability of the disease-free equilibrium E_f.

About the numerical simulations concerning the stability of the two endemic equilibria, we have the following results: First, Fig. 4.2 shows the behavior of the infection for the first 100 days of observation for the problem parameters corresponding to the immune-free equilibrium stability. The chosen parameters in this figure ensure that the basic reproduction number is greater than unity ($R_0=11.049>1$) and the immune response reproduction number is less than unity ($R_{CTL}=3.596\times10^{-1}<1$). It is clearly seen that, in this case, all the solutions converge towards the immune-free endemic equilibrium $E_1=(19.96,5.98\times10^{-1},1.14,199.78,0)$ which agrees with our theoretical finding concerning the stability of the first endemic equilibrium E_1. This absence of effective CTL activity can lead to uncontrolled viral replication, persistent infection, and increased pathogenicity. Finally, Fig. 4.3 illustrates the disease dynamics when both the basic reproduction number and the immune response reproduction number are greater than unity. Indeed, for the chosen parameters in this figure, we have $R_0=11.049>1$ and $R_{CTL}=4.13>1$. It can be seen that the infection persists and the convergence towards the infection steady state

Table 1: Parameters, their symbols and default values used in the suggested viral model

Parameters	Meaning	Value	References
λ	Source rate of uninfected cells	$[0,10]$	[16]
k_1	Average of infection	$[2.5\times10^{-4},0.5]$	[16]
d_1	Decay rate of healthy cells	0.0139	[16]
d_2	Death rate of exposed cells	0.0495	[16]
k_2	The rate that exposed become infected cells	1.1	[16]
d_3	Death rate of infected cells, not by CTL killing	0.5776	[16]
a	The rate of production the virus by infected cells	$[2,1250]$	[16]
d_4	Clearance rate of virus	$[0.3466,2.4]$	[16]
p	Clearance rate of infection	0.0024	[16]
c	Activation rate CTL cells	0.15	[16]
b	Death rate of CTL cells	0.5	[16]

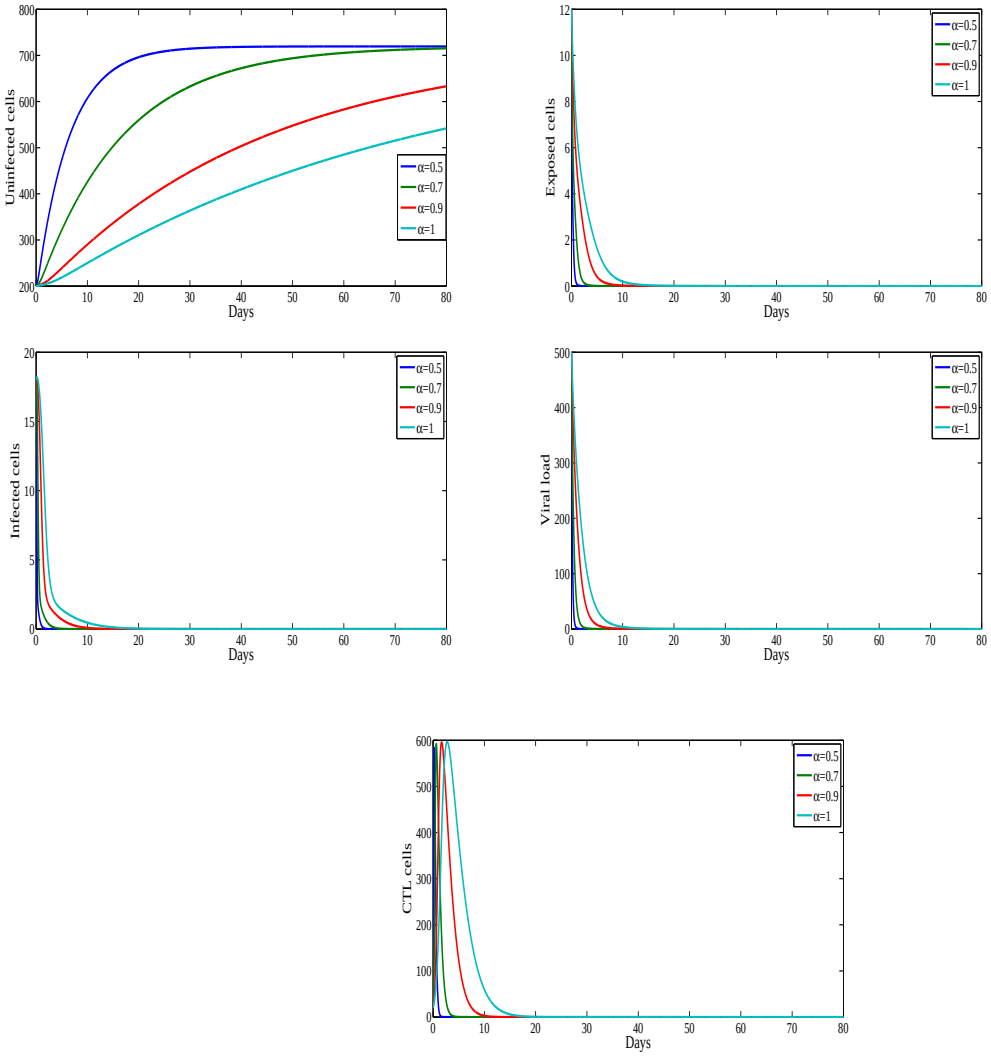

Figure 4.1: The dynamics of the viral infection when $\lambda = 10$, $d_1 = 0.0139$, $k_1 = 0.04$, $d_2 = 0.0495$, $k_2 = 1.1$, $d_3 = 0.5776$, $a = 2$, $d_4 = 0.6$, $p = 0.0024$, $c = 0.15$, $b = 0.5$.

$E_3 = (285.12, 6.55, 3.33, 555.55, 660.86)$ is observed. We note that from the three previous numerical results, the order of the fractional derivative α has no effect on the stability of the three equilibria. However, for higher values of α, which describes the long memory behavior, the solutions converge more quickly to the steady states. The presence of a robust cytotoxic T lymphocyte (CTL) response is crucial for controlling viral infections. An effective CTL response helps limit viral replication, facilitates the clearance of infected cells, and reduces the likelihood of persistent infection and disease progression. This immune activity is a key factor in the resolution of many acute viral infections and contributes significantly to the overall antiviral defense. Enhancing CTL responses remains a central goal in the development

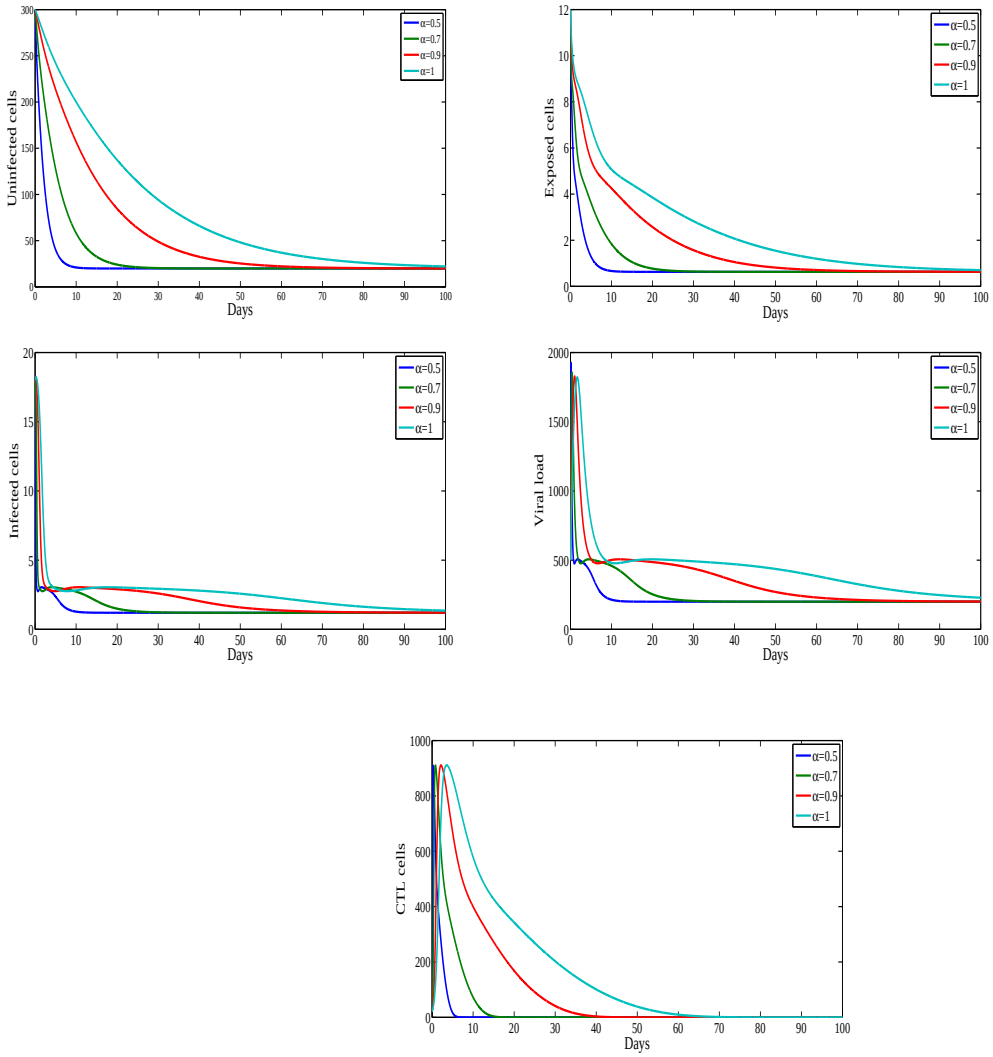

Figure 4.2: The evolution of the viral infection for $\lambda = 1$, $d_1 = 0.0139$, $k_1 = 0.04$, $d_2 = 0.0495$, $k_2 = 1.1$, $d_3 = 0.5776$, $a = 100$, $d_4 = 0.6$, $p = 0.0024$, $c = 0.15$, $b = 0.5$.

of vaccines and immunotherapies.

5. Conclusion

In this paper, the dynamics of the viral infection model is studied by taking into account the memory effect. The Caputo fractional derivative and the cellular immunity are taken into consideration in the mathematical formulation of the model. The positivity and boundedness of solutions are proved. Moreover, it has been established that the proposed model has three steady states, namely, the disease-free equilibrium E_f, the infection steady state without cellular immunity E_1 and the infection steady state with cellular immunity E_2. The global stability of the disease-free equilibrium and the endemic equilibria are established. Finally, some numerical simulations are presented in order to support the theoretical findings. Both the theoretical and the numerical results reveal that the order of the fractional derivative α has no effect on the steady states stability. Moreover, for higher values of α, which describes the long memory behavior, the solutions converge more quickly to the steady states. This result can be explained by the memory term $\frac{1}{\Gamma(1-\alpha)(t-u)^{\alpha}}$ included in the fractional derivative which represents the time needed for the interaction between cells and viral particles and the time needed for the activation of the cellular immune response. These findings highlight the usefulness of incorporating fractional-order calculus into infectious disease modeling. The ability of the model to reflect memory-dependent biological processes, such as delayed immune responses or prolonged infection stages, provides a more realistic framework compared to classical models. Furthermore, the proposed numerical simulations offer valuable insights into how memory effects influence the system's dynamic behavior over time. They also demonstrate the flexibility and robustness of the fractional-order model in simulating different scenarios of viral dynamics under varying immune conditions. Such insights can be instrumental in guiding therapeutic strategies and improving understanding of immune system-virus interactions.

Article Information

Acknowledgements: I would like to express my gratitude to my supervisor Dr. Zakir Deniz for his guidance and invaluable comments. I also thank the referees for their valuable suggestions and for carefully reviewing the manuscript.

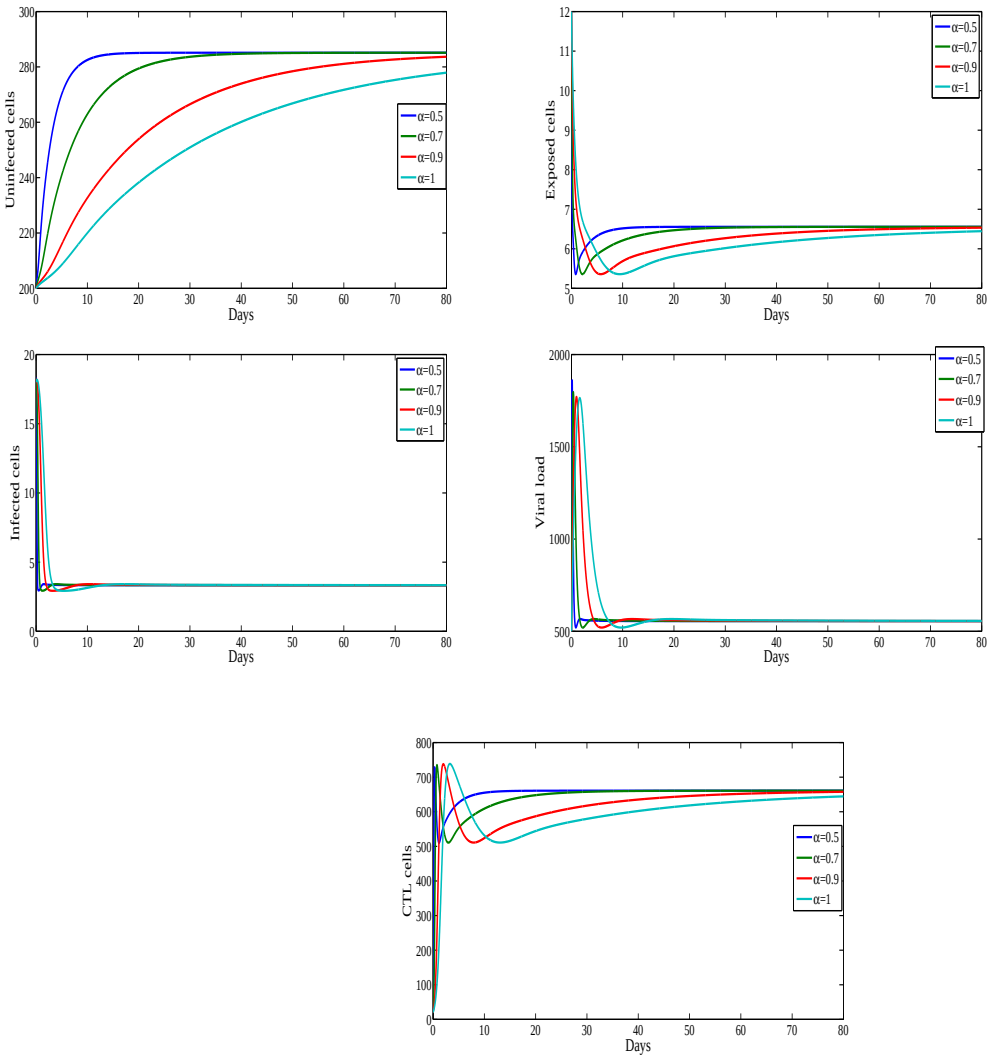

Figure 4.3: The behavior of the viral infection for $\lambda = 10$, $d_1 = 0.0139$, $k_1 = 0.04$, $d_2 = 0.0495$, $k_2 = 1.1$, $d_3 = 0.5776$, $a = 100$, $d_4 = 0.6$, $p = 0.0024$, $c = 0.15$, $b = 0.5$.

Author's contributions: All authors contributed equally to the writing of this paper. All authors read and approved the final manuscript.

Conflict of Interest Disclosure: No potential conflict of interest was declared by the author.

Copyright Statement: Authors own the copyright of their work published in the journal and their work is published under the CC BY-NC 4.0 license.

Supporting/Supporting Organizations: No grants were received from any public, private or non-profit organizations for this research.

Ethical Approval and Participant Consent: It is declared that during the preparation process of this study, scientific and ethical principles were followed and all the studies benefited from are stated in the bibliography.

Plagiarism Statement: This article was scanned by the plagiarism program. No plagiarism detected.

Availability of data and materials: Not applicable

References

[1] World Health Organization, HIV/AIDS key facts, Available from *https://www.who.int/topics/infectious diseases/en/index.html*.
[2] Maziane, M., Lotfi, E. M., Hattaf, K., Yousfi, N. (2015). Dynamics of a class of HIV infection models with cure of infected cells in eclipse stage. Acta Biotheoretica, 63(4), 363-380.
[3] Shi, V., Tridane, A., Kuang, Y. (2008). A viral load-based cellular automata approach to modeling HIV dynamics and drug treatment. Journal of theoretical biology, 253(1), 24-35.
[4] Wodarz, D. Hepatitis C virus dynamics and pathology: The role of CTL and antibody responses. J. Gen. Virol. 2003, 84, 1743–1750.
[5] Li, M.; Zu, J. The review of differential equation models of HBV infection dynamics. J. Virol. Methods 2019, 266, 103–113.
[6] Danane, J., Meskaf, A., Allali, K. (2018). Optimal control of a delayed hepatitis B viral infection model with HBV DNA-containing capsids and CTL immune response. Optimal Control Applications and Methods, 39(3), 1262-1272.
[7] Burchell, A.N.; Winer, R.L.; de Sanjosé, S.; Franco, E.L. Epidemiology and transmission dynamics of genital HPV infection. Vaccine 2006, 24, S52–S61.
[8] Elbasha, E.H.; Dasbach, E.J.; Insinga, R.P. A multi-type HPV transmission model. Bull. Math. Biol. 2008, 70, 2126–2176.

[9] Braaten, K. P., Laufer, M. R. (2008). Human papillomavirus (HPV), HPV-related disease, and the HPV vaccine. Reviews in obstetrics and gynecology, 1(1), 2.

[10] Nowak M.A.; Bangham C.R.M. Population dynamics of immune responses to persistent viruses. *Science* **1996**, *272*, 74–79.

[11] Smith H.L.; De Leenheer P. Virus dynamics: a global analysis. *SIAM Journal on Applied Mathematics* **2003**, *63*, 1313-1327.

[12] Korobeinikov A. Global properties of basic virus dynamics models. *Bulletin of Mathematical Biology* **2004**, *66*, 879–883.

[13] Buonomo, B., Vargas-De-Le´on, C.(2012) Global stability for an HIV-1 infection model including an eclipse stage of infected cells, J. Math. Anal. Appl.385(2):709-720.

[14] Sun Q.; Min L.; Kuang Y. Global stability of infection-free state and endemic infection state of a modified human immunodeficiency virus infection model. *IET systems biology* **2015**, *9*, 95–103.

[15] Sun Q.; Min L. Dynamics Analysis and Simulation of a Modified HIV Infection Model with a Saturated Infection Rate. *Computational and mathematical methods in medicine* **2014**, *2014* Article ID 145162, 14 pages.

[16] Allali, K., Danane, J., Kuang, Y., 2017. Global Analysis for an HIV Infection Model with CTL Immune Response and Infected Cells in Eclipse Phase. Applied Sciences (2076-3417), 7(8).

[17] Raeisi, E., Yavuz, M., Khosravifarsani, M., & Fadaei, Y. (2024). Mathematical modeling of interactions between colon cancer and immune system with a deep learning algorithm. The European Physical Journal Plus, 139(4), 345.

[18] Wang X.; Tao Y.; Song X. Global stability of a virus dynamics model with Beddington-DeAngelis incidence rate and CTL immune response. *Nonlinear Dynamics* **2011**, *66*, 825–830.

[19] Daar, E.S.; Moudgil, T.; Meyer, R.D.; Ho, D.D. Transient high levels of viremia in patients with primary human immunodeficiency virus type 1. N. Engl. J. Med. 1991, 324, 961–964.

[20] Naim, M., Zeb, A., Mohsen, A. A., Sabbar, Y., & Yıldız, M. (2024). Local and global stability of a fractional viral infection model with two routes of propagation, cure rate and non-lytic humoral immunity. Mathematical Modelling and Numerical Simulation with Applications, 4(5-Special Issue: ICAME'24), 94-115.

[21] Joshi, H., Yavuz, M., Taylan, O., & Alkabaa, A. (2025). Dynamic analysis of fractal–fractional cancer model under chemotherapy drug with generalized Mittag-Leffler kernel. Computer Methods and Programs in Biomedicine, 260, 108565.

[22] Kahn, J.O.; Walker, B.D. Acute human immunodeficiency virus type 1 infection. N. Engl. J. Med. 1998, 339, 33–39.

[23] Sokolov IM, Chechkin AV, Klafter J. Distributed-order fractional kinetics. Statistical Physics: Fundamentals and Applications 2004; 35:1323–1341.

[24] Rida SZ, El-Sayed AMA, Arafa AM. A effect of bacterial memory dependent growth by using fractional derivatives reaction-diffusion chemotactic model. Journal of Statistical Physics 2010; 140:797–811.

[25] Arafa AAM, Rida SZ, Khalil M. Fractional modeling dynamics of HIV and CD4CT -cells during primary infection. Nonlinear Biomedical Physics 2012; 6(1).

[26] Sweilam NH, AL-Mekhlafi SM. Numerical study for multi-strain tuberculosis (TB) model of variable-order fractional derivatives. Journal of Advanced Research 2016; 7(2):271–283.

[27] A. Boukhouima, K. Hattaf, and N. Yousfi, Dynamics of a Fractional Order HIV InfectionModel with Specific Functional Response and Cure Rate, International Journal of Differential Equations, vol. 2017, Article ID 8372140, 8 pages, 2017.

[28] Debnath L. Recent applications of fractional calculus to science and engineering. International Journal of Mathematics and Mathematical Sciences 2003; 54:3413–3442.

[29] Hilfer ER. Applications of Fractional Calculus in Physics. World Scientific: River Edge, NJ, USA, 2000.

[30] Yuste SB, Acedo L, Lindenberg K. Reaction front in a reaction-subdiffusion process. Physical Review E 2004; 69:036126-1–036126-10.

[31] Lin W. Global existence theory and chaos control of fractional differential equations. Journal of Mathematical Analysis and Applications 2007; 332:709–726.

[32] Sheng H, Chen YQ, Qiu TS. Fractional Processes and Fractional-order Signal Processing. Springer: New York, NY, USA, 2012.

[33] Ferdi Y. Some applications of fractional order calculus to design digital filters for biomedical signal processing. Journal of Mechanics in Medicine and Biology 2012; 12:1–13.

[34] Chen W-C. Nonlinear dynamics and chaos in a fractional-order financial system. Journal of Chaos, Solitons and Fractals 2008; 36:1305–1314

[35] Naik, P. A., Yeolekar, B. M., Qureshi, S., Yavuz, M., Huang, Z., & Yeolekar, M. (2025). Fractional insights in tumor modeling: an interactive study between tumor carcinogenesis and macrophage activation. Advanced Theory and Simulations, 2401477.

[36] Manivel, M., Venkatesh, A., & Kumawat, S. (2025). A comprehensive study of monkeypox disease through fractional mathematical modeling. Mathematical Modelling and Numerical Simulation with Applications, 5(1), 65-96.

[37] Naik, P. A., Yavuz, M., Qureshi, S., Owolabi, K. M., Soomro, A., Ganie, A. H. (2024). Memory impacts in hepatitis C: A global analysis of a fractional-order model with an effective treatment. Computer Methods and Programs in Biomedicine, 254, 108306.

[38] Jha, B. K., Vora, H., & Singh, T. P. (2024). The effect of amyloid beta, membrane, and ER pathways on the fractional behavior of neuronal calcium. Bulletin of Biomathematics, 2(2), 198-217.

[39] Yavuz, M., Akman, M., Usta, F., & Özdemir, N. (2022, November). Effect of the awareness parameter on a fractional-order tuberculosis model. In AIP Conference Proceedings (Vol. 2483, No. 1). AIP Publishing.

[40] Evirgen, F., Özköse, F., Yavuz, M., & Özdemir, N. (2023). Real data-based optimal control strategies for assessing the impact of the Omicron variant on heart attacks. AIMS Bioengineering, 10(3).

[41] Joshi, H., & Yavuz, M. (2025). Chaotic dynamics of a cancer model with singular and non-singular kernel. Discrete and Continuous Dynamical Systems-S, 18(5), 1416-1439.

[42] Nguefack, D. J. T. (2024). Mathematical modeling of schistosomiasis transmission using reaction-diffusion equations. Fundamental Journal of Mathematics and Applications, 7(2), 118-136.

[43] Eğilmez Hİ, Haspolat E. (2024) Temperature-Dependent Parameters in Enzyme Kinetics: Impacts on Enzyme Denaturation. Fundamental Journal of Mathematics and Applications, 7(4), 226-235.

[44] Yavuz, M., Özdemir, F. N., Akyüz, K., & Bayraktar, N. B. The relationship between colon cancer and immune system: a fractional order modelling approach. Balıkesir Üniversitesi Fen Bilimleri Enstitüsü Dergisi, 27(1), 126-144.

[45] Iwa, L. L., Omame, A., & Inyama, S. C. (2024). A fractional-order model of COVID-19 and Malaria co-infection. Bulletin of Biomathematics, 2(2), 133-161.